GA–A26109

EXPERIMENTS TO MEASURE HYDROGEN RELEASE FROM GRAPHITE WALLS DURING DISRUPTIONS IN DIII-D

by
E.M. HOLLMANN, N.A. PABLANT, D.L. RUDAKOV,
J.A. BOEDO, N.H. BROOKS, T.C. JERNIGAN,
and A.YU. PIGAROV

JUNE 2008

GENERAL ATOMICS

DISCLAIMER

GA–A26109

EXPERIMENTS TO MEASURE HYDROGEN RELEASE FROM GRAPHITE WALLS DURING DISRUPTIONS IN DIII-D

by
E.M. HOLLMANN,* N.A. PABLANT,* D.L. RUDAKOV,*
J.A. BOEDO,* N.H. BROOKS, T.C. JERNIGAN,†
and A.YU. PIGAROV*

This is a preprint of a paper to be presented at the Eighteenth International Conference on Plasma Surface Interactions, May 26-30, 2008, in Toledo, Spain, and to be published in J. Nucl. Mater.

*University of California-San Diego, California
†Oak Ridge National Laboratory, Oak Ridge, Tennessee

Work supported by
the U.S. Department of Energy
under DE-FC02-04ER54698, DE-FG02-07ER54917
and DE-AC05-00OR22725

GENERAL ATOMICS ATOMICS PROJECT 30200
JUNE 2008

GENERAL ATOMICS

ABSTRACT

Spectroscopy and wall tile bake-out measurements are performed in the DIII-D tokamak to estimate the amount of hydrogen stored in and released from the walls during disruptions. Both naturally occurring disruptions and disruptions induced by massive gas injection (MGI) are investigated. The measurements indicate that both types of disruptions cause a net release of order 10^{21} hydrogen (or deuterium) atoms from the graphite walls. This is comparable to the pre-disruptions plasma particle inventory, so the released hydrogen is important for accurate modeling of disruptions. However, the amount of hydrogen released is small compared to the total saturated wall inventory of order $10^{22}-10^{23}$, so it appears that many disruptions are necessary to provide full pump-out of the vessel walls.

1. INTRODUCTION

Hydrogen and its isotopes are the primary working gases in tokamak experiments, so storage and release of hydrogen from the plasma-facing components (PFCs) has an important effect on tokamak fueling and density control [1]. In future tokamaks, understanding of hydrogen retention in PFCs will become even more crucial, due to the need to track tritium for fueling and safety considerations. Because of its excellent resistance to high heat fluxes, graphite is frequently used as a PFC, and its behavior in hydrogen has been studied extensively. Under hydrogenic plasma fluxes typical to tokamaks, graphite PFCs are found to saturate rapidly (within 10-100 ms) with hydrogen. The saturated layer typically has a deposition depth of order 50 nm and hydrogen content H/C $\approx 0.4/1$, giving area densities of order 10^{21} H atoms/m^2 [2]. Over longer time periods, co-deposition of sputtered C and H in cold PFC regions of net deposition can result in much thicker layers, with co-deposited H/C layers of up to 1 mm in thickness being reported [3].

Very little is known about the release, migration, and re-deposition of PFC materials during fast transient events such as edge-localized modes (ELMs) and disruptions. During these events, plasma-wall fluxes can increase by many orders of magnitude over quiescent levels, possibly causing a significant change in erosion/deposition patterns. A large transient release of both carbon [4] and stored hydrogen [5] has been inferred indirectly on the DIII-D tokamak during disruptions, and the use of disruptions as a wall cleaning technique was attempted in TFTR [6]. Use of disruptions initiated by massive gas injection (MGI) as a method to remove tritium/carbon co-deposits in ITER has been suggested [7].

In the work presented here, measurements of hydrogen release from the walls of DIII-D during disruptions are presented. Two types of disruptions are studied: “naturally” occurring disruptions which arise during normal operation due to hardware malfunctions or performance limits, and disruptions induced intentionally by MGI (either hydrogen or neon). Overall, the measurements indicate a net release of order 10^{21} H particles during all types of disruptions; this is about the same size as the plasma particle inventory, but small compared with the total wall inventory ($\approx 10^{23}$ H particles). Ne MGI is observed to preferentially release main chamber H particles from the wall, while H_2 MGI tends to release more H from the divertor region.

2. EXPERIMENT HARDWARE

A cross section view of DIII-D and schematics of some diagnostics used here is shown in Fig. 1. Most of the experiments discussed here used lower-single null H-mode discharges. All used D_2 as a fuel gas. A radially viewing CO_2 interferometer chord was used to measure plasma density during the disruptions. For the MGI-induced disruptions, a single fast valve was used to inject gas into the discharge. Either H_2 (about 1500 Torr-l$\approx 10^{23}$ H atoms in a 5 ms pulse) or Ne (about 1000 Torr-l$\approx 3\times10^{22}$ Ne atoms in a 10 ms pulse) was used. To measure wall recycling of H and D, a slow (100 ms) high-resolution divertor spectrometer with six view chords across the lower divertor and two view chords across the main chamber was used, as was a fast (0.3 ms), single-chord spectrometer. Additionally, in one MGI experiment, the DiMES sample manipulator [8] was used to insert an $A = 18$ cm^2 graphite sample into the divertor floor.

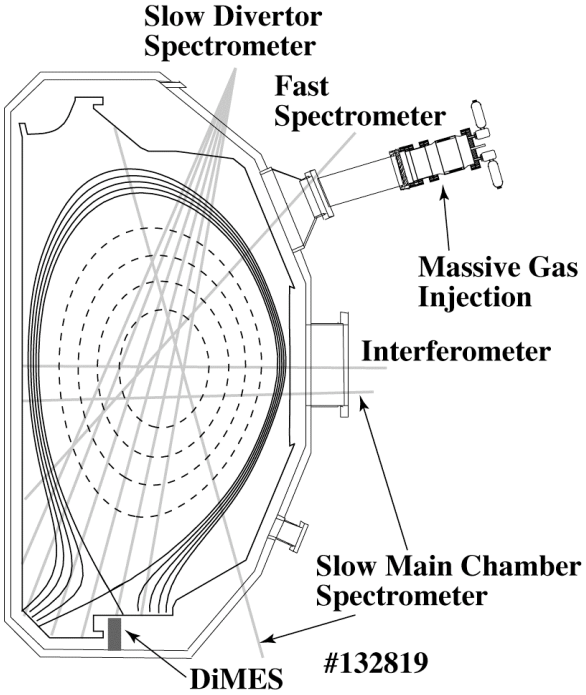

Fig. 1. DIII-D cross section showing main diagnostics used in this work.

3. NATURAL DISRUPTIONS

Disruptions are characterized by a fast (~1 ms) thermal quench (TQ) phase where most of the plasma thermal energy is lost (often mostly to the divertor), followed by a slower (~ 5 ms) current quench (CQ) phase where the plasma magnetic energy is lost (often mostly to the main chamber). Electron density measurements taken during natural disruptions indicate that a significant transient release of particles into the plasma occurs during the disruptions. Figure 2 shows the initial (pre-disruption) and peak (usually slightly after end of TQ) electron number measured with the interferometer. Disruptions which occurred during the operation period Jan – Feb of 2007 are shown. Although there is a significant scatter in the data, it can be seen that, on average, there is an increase of order 2–4× in the plasma electron number (i.e. an increase of about 10^{21} electrons). An increasing trend with increasing plasma thermal energy is seen, i.e., higher energy plasma tend to both store more electrons in the discharge and release more electrons from the wall when they disrupt.

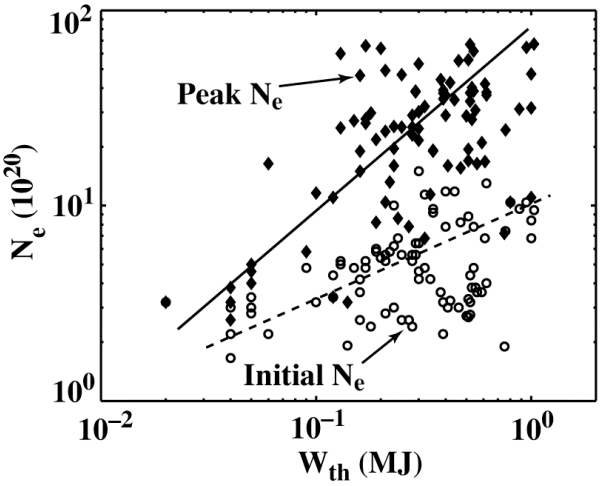

Fig. 2. Initial and peak plasma electron number during natural disruptions as a function of initial plasma thermal energy W_{th}.

0D modeling suggests that the observed increase in electron number comes dominantly from deuterium. During the TQ phase, the plasma is very anisotropic, with strong temperature and density gradients; however, in the CQ phase, the plasma is more well-mixed, and 0D modeling of the plasma current decay is found to be reasonably successful at matching average plasma parameters. An example of this is shown in Fig. 3, where data and modeling of a natural disruption is shown. In the model, the plasma is initialized with the measured mean values of electron density n_e, electron temperature T_e, ion temperature T_i, and plasma current I_p. The measured initial carbon content of 2% is included; this is assumed to be entirely C^{6+}. The model unknowns are the rates of conducted heat loss to the walls, net rate of deuterium influx from the

walls, and net rate of carbon influx from the walls; all these are assumed to be proportional to the plasma thermal energy W_{th}, with the three normalization constants varied as free parameters. The disruption simulation begins at time t_0. Charge-state resolved, non-equilibrium atomic physics (ionization, recombination, and radiation) including radiation trapping are included in the simulation [9]. The electron distribution is assumed to be Maxwellian, so runaway electron formation is neglected. Overall, it is found that matching the observed radiated power P_{rad} requires the addition of a small amount of sputtered carbon ($\approx 10^{20}$ C atoms). However, this added carbon does not cause n_e increase to match the data; for this, the addition of significant amounts of deuterium ($\approx 10^{21}$ D atoms) is required. This can be seen in Fig. 3(c), where the deuterium ion density n_D is seen to be more that $10\times$ larger than the carbon ion density n_C. Although recycling is ignored in the model (atoms added from the wall are assumed to remain in the plasma), it is expected that inclusion of recycling will not invalidate the need for a deuterium source term in the 0D modeling, since recycling produces no net increase in n_e. However, since recycling will allow each D to radiate more often, it is possible that the amount of carbon influx needed to match P_{rad} in reality is less than predicted by the modeling. The small ~ 1 ms timing differences seen between modeling and experiment ([e.g. in T_e Fig. 3(a)] are thought to be due to 1D (radial transport) delays and do not significantly affect the conclusions drawn here.

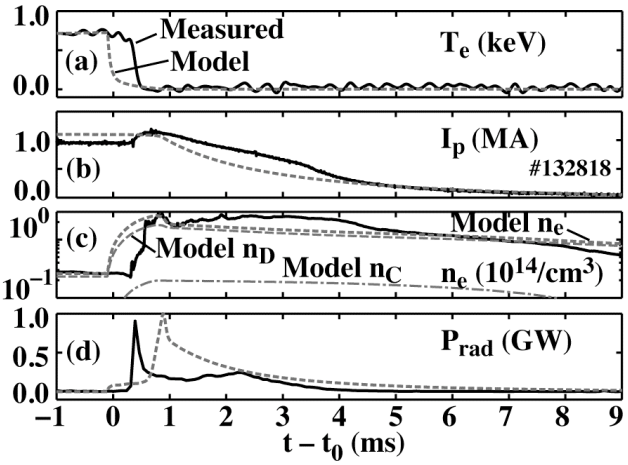

Fig. 3. Time traces of a natural disruption (solid lines) and 0D modeling (dashed lines) for (a) average electron temperature T_e, (b) plasma current I_p, (c) average electron density n_e (including modeled deuterium and carbon ion densities n_D and n_C), and (d) radiated power P_{rad}.

4. MGI-INDUCED DISRUPTIONS

To study wall release of hydrogen during MGI disruptions, a series of shots were shut down with MGI: two with H_2 MGI followed by four with Ne MGI. Initial (pre-disruption) wall conditions are not measured independently in these experiments; however, based on previous experience [5], we expect the walls to contain of order $10^{22}-10^{23}$ deuterons before the first MGI disruption. Divertor hydrogen fluxes measured with the divertor spectrometer over the series of shots are shown in Fig. 4. The time axis shows cumulative shot time ignoring dead time between shots. Vertical gray lines show MGI shutdown times. Total hydrogen fluxes shown in Figs. 4(a) and 4(b) are estimated from H_γ and D_γ brightness (at 434 nm) while total hydrogen fluxes from hydrocarbons shown in Fig. 4(c) are estimated from CH and CD brightness (with band heads around 431 nm). Rough conversions from measured brightness to hydrogen fluxes plotted in Fig. 4 are made using typical photon efficiency conversions for attached conditions ($S/XB \approx 1000$ for H_γ, D_γ [10], $(D/XB)^{CD_4 \rightarrow CD} \approx 40$ for CD and $(D/XB)^{CH_4 \rightarrow CH} \approx 30$ for CH [11]). Fluxes are integrated over the lower divertor area (≈ 6 m^2) to estimate divertor inflow or over the plasma surface area (≈ 20 m^2) to estimate main chamber inflow. Despite the qualitative nature of these estimates, several interesting trends can be seen in the data. Hydrogenic fluxes/recycling in the divertor can be seen to be much ($> 10\times$) larger during H_2 MGI than Ne MGI. Following a single H_2 MGI disruption, a large H wall inventory is achieved, with comparable H versus D fluxes in both divertor and main chamber seen during normal operation in the subsequent shot (before the disruption). Suprisingly, divertor hydrocarbon emission remains relatively small and unaffected both during and after the disruptions. For example, CH emission is much smaller than CD after the H_2 MGI, even though total H flux appears to be comparable. Although the H_2 MGI is clearly quite effective at embedding H_2 into the walls, the Ne MGI does not appear to be especially effective at removing PFC hydrogen. In shots #132821 - #132824, a gradual decrease of divertor H emission (relative to D) during the shots can be seen; however, there is only one clear indication of stepwise decrease in the H/D ratio following Ne MGI: this is after shot #132823, where a significant (almost $2\times$) drop in main chamber H fraction is observed.

In the data of Fig. 4, the spectrometer integration time was 100 ms and therefore integrates over both the TQ and CQ phases of the disruptions. This complicates interpretation of the data during the disruption since, for example, H_γ is expected to correspond dominantly to ionization radiation during the TQ and recombination radiation during the CQ. Separation of the TQ and CQ times was obtained with a single-chord fast spectrometer (dominantly viewing the main chamber). Figure 5 shows (a) electron number N_e from the interferometer and (b) H_α and D_α emission measured with the fast spectrometer. In this shot #132819, the walls were initially loaded only with D, and the plasma contained about 5×10^{20} deuterium ions. At $t = 2000$ ms the shot was shut down with H_2 MGI. In the middle of the CQ phase ($t \approx 2006-2010$ ms), where the plasma is expected to be reasonably well-mixed, the deuteron number in the plasma N_D can

be estimated from the measured D_α fraction: $N_D \approx N_e (D_\alpha / D_\alpha + H_\alpha)$. This is shown with the gray curve in Fig. 5(a). Overall, the data suggest $N_D \approx 10^{21}$ during the CQ, consistent with a net release of about 5×10^{20} deuterons from the wall, probably mostly during the TQ, where the largest rise in N_e is seen.

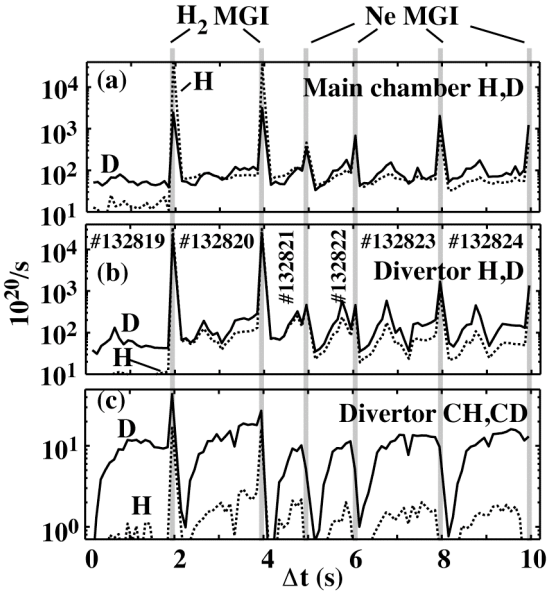

Fig. 4. Hydrogen recycling inflow measured spectroscopically (a) in the main chamber by H_γ, D_γ brightness; (b) in the divertor by H_γ, D_γ ; and in the divertor by CH, CD. Six discharges are shown, each terminated with MGI. The time axis shows cumulative discharge time Δt.

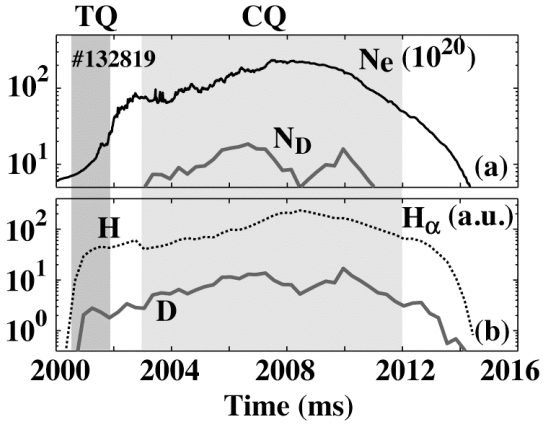

Fig. 5. (a) Measured electron number N_e (black curve) and deuterium ion number estimated from (b) measured H_α and D_α brightness. Shaded regions mark thermal quench (TQ) and current quench (CQ).

To measure the amount of deuterium stored in the graphite wall directly, a graphite sample was inserted using the DiMES sample manipulator. Two separate exposures were performed: in the first, the sample was exposed to three normal D_2 discharges, transferred under argon to a bake-out chamber and baked out at 1000°C for 1.5 h to measure the deuterium content (seen as HD and D_2 in an RGA). In the second exposure, the sample was again exposed to three D_2 discharges, the last of which was terminated with H_2 MGI. The bake-out pressure traces of the two samples, shown in Fig. 6, are seen to be fairly similar. A calibrated D_2 leak was used to

calibrate the pressure traces, giving about 3.7×10^{18} D atoms in the MGI case and 2.0×10^{18} D atoms in the non-MGI case; this small variation is probably within the shot-shot variation, so we conclude that the net D release from H_2 MGI is relatively small. Hydrogen background levels in the bake-out chamber were too large to accurately measure H_2 stored in the samples.

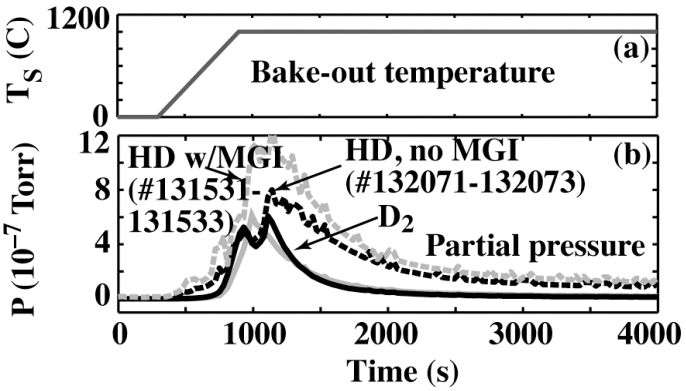

Fig. 6. Bake-out traces of graphite DiMES samples exposed to D_2 discharges with (gray) and without (black) H_2 MGI, showing partial pressure of HD (dashed curves) and D_2 (solid curves).

5. DISCUSSION

The area density of D measured with the DiMES bake-out after only three shots exposure ($\approx 1.7\times10^{21}$ D/m^2) is consistent with expected saturation densities ($\approx 10^{21}$ D/m^2) and, multiplied by the wall area of 70 m^2, gives a wall inventory $\approx 10^{23}$ consistent with pumping measurements in DIII-D [5]. Assuming only the divertor wall region is saturated with D, the wall inventory is still quite large, $\approx 10^{22}$. During disruptions, very large recycling fluxes are observed, but a surprisingly small fraction (~ 1%) of the wall inventory is ultimately lost and pumped away. For example, in H_2 MGI disruptions, of order 10^{23} hydrogen atoms are injected into the vacuum chamber and recycling inflows of order 10^{23} are observed in both main chamber and divertor (as seen in Fig. 4 taking 10^{24}/s times 0.1 s integration time). These large hydrogen fluxes appear to be dominantly recycled and redeposited though, and do not appear to result in a large net loss of D from the wall, with a net $\approx 10^{21}$ deuterons lost from the wall suggested in Fig. 5(a) and no net loss of D seen in Fig. 6. Hydrogen implantation appears to be easier than hydrogen removal, as after a single H_2 MGI shot, the PFC H/D ~ 1, with the ratio still being H/D ~1/2 after several shots terminated with Ne MGI disruptions, Fig. 4(b). For MGI disruptions, recycling fluxes appear to be larger in the divertor for H_2 MGI and larger in the main chamber for Ne MGI. There is some evidence for net removal of D from the main chamber following Ne MGI. Chemical erosion as measured by CD emission (which is thought to arise dominantly as a result of CD_4 emission) does not appear to be significantly affected by MGI disruptions, nor does it appear to account for the measured release of hydrogen during the disruptions. Overall, these measurements indicate that PFC release of hydrogen is important for accurate modeling of disruptions in tokamaks with graphite walls. MGI-induced disruptions do not appear to be highly efficient at cleaning existing hydrogen out of PFCs; although they may serve as a useful complement to other wall cleaning techniques.

REFERENCES

[1] J. Winter, Plasma Phys. Contr. Fusion 36 (1994) B263.

[2] G. Federici, C.H. Skinner, J.N. Brooks, et al., Nucl. Fusion 41 (2001) 1968.

[3] M. Mayer, V. Phillips, P. Wienhold, et al., J. Nucl. Mater. 290 (2001) 381.

[4] E.M. Hollmann, D.S. Gray, D.G. Whyte, et al., Phys. Plasmas 10 (2003) 2863.

[5] R. Maingi, G.L. Jackson, M.R. Wade, et al., Nucl. Fusion 36 (1996) 245.

[6] H.F. Dylla, et al., J. Nucl. Mater. 145 (1987) 48.

[7] D.G. Whyte and J.W. Davis, J. Nucl. Mater. 337 (2005) 560.

[8] C.P.C. Wong, D.L. Rudakov, J.P. Allain, et al., J. Nucl. Mater. 363 (2007) 276.

[9] E.M. Hollmann et al., "Measurements of injected impurity assimilation during massive gas injection experiments in DIII-D," submitted to Nucl. Fusion (2008).

[10] R.K. Janev, D. Reiter, and U. Samm, "Collision processes in low-temperature hydrogen plasmas," (Jul-4105, Forzchungszentrum Juelich, 2003).

[11] S. Brezinsek, A. Pospieszczk, D. Borodin, et al., J. Nucl. Mater. 363 (2007) 1119.

ACKNOWLEDGMENT

This work supported by the U.S. Department of Energy under DE-FC02-04ER54698, DE-FG02-07ER54917 and DE-AC05-00OR22725. Assistance of Drs. M. Baldwin, J. Hanna, G. Temmerman, and K. Umstader in using the PISCES lab TDS system is acknowledged.